Journal of Textile Science & Engineering

Research Article

Li-doped ZnO Sol-Gel Thin Films: Correlation between Structural Morphological and Optical Properties

Wannes HB[1,3]*, Dimassi WR[1], Zaghouani B[1] and Mendes MJ[2]

[1]Photovoltaic Laboratory, Center for Research and Energy Technologies, Borj-Cedria Technopole, Tunisia
[2]Department of Materials Science, Faculty of Science and Technology, NOVA University of Lisbon and CEMOP/UNINOVA, Campus of Caparica, Lisbon, Portugal
[3]Faculty of Sciences of Tunis, Tunis El Manar University, Tunis, Tunisia

Abstract

Transparent Conducting Oxides (TCOs) have important device applications used in solar cells as transparent electrodes. In particular, ZnO material has been investigated for many years due to its excellent physical properties and potential applications in transparent conductive contacts when it is doped by several types of doping. If n-type doping is easily achievable in ZnO, the realization of stable and reproducible p-type ZnO is still difficult. The group I (Li, Na) atoms could be potential candidates to result in p-type ZnO. The choice of lithium as a dopant is motivated firstly by its abundance in nature, its low cost compared to other alkali metals and its wide application. Undoped and Lithium-doped zinc oxide thin films (ZnO:Li) at different percentages (5, 15 and 25%) were prepared on glass substrates, using the sol–gel spin-coating method, and the influence of the Li concentration on the structural, morphological and optical properties of the ZnO thin films was investigated. X-ray diffraction (XRD) analysis shows that the un-doped and 5 at % Li-doped films have a hexagonal wurtzite structure and are preferentially oriented along the c-axis from the substrate. SEM analysis shows a compact surface with mainly hexagonal grains. Optical transmittance measurements show that all samples have average 88% transparency in the visible light, with a sharp fall of the absorption at a wavelength (~376 nm) close to the ZnO band gap. The results suggest that the optical properties of the ZnO:Li films can be further improved for solar cell applications.

Introduction

Recently, Zinc Oxide (ZnO) has attracted much interest and has been proposed as an alternative to indium tin oxide (ITO) used as a transparent conducting oxide (TCO). Unlike ITO in which indium is considered as a rare earth metal, zinc oxide is an inexpensive semiconductor. Moreover, it is non-toxic and may occur under many forms such as bulk crystal, powder, thin film, nanowires and nanotubes. ZnO is one of the most important II-VI wide band gap (WBG) semiconducting material with a band gap around 3.37 eV at room temperature crystallizing in hexagonal Wurtzite structure. Specially, ZnO thin films are widely studied to be integrated in optoelectronics devices such as solar cells thanks to a large exciton binding energy of 60 meV [1]. The photovoltaic devices based on zinc oxide (ZnO) thin films are more stable when exposed to hydrogen plasma unlike to the SnO_2 and ITO whose the optical transmission is deteriorated under hydrogen plasma [2,3].

ZnO thin films could be grown on different substrates by numerous techniques: sputtering, Chemical Vapor Deposition, Laser Ablation, Spray pyrolysis, sol-gel spins coating [4-9]. Intrinsic ZnO thin films are found to be n-type semiconductor with electron concentration depending on the deposition method and parameters. Zaharescu et al. have reported on undoped ZnO elaborated by sol-gel technique exhibiting n-type conduction with a low carrier concentration of $5.48.10^{14}$ cm^{-3}[10]. The n-type conduction is justified by the presence of defects like oxygen Vacancies (V_0) and interstitial zinc (Zn_i) [11]. The electrical properties of zinc oxide can be ameliorated by an appropriate n or p-type doping. The characteristic features of doped ZnO thin films are their high carrier concentration and low mobility and their transparency to the visible light making it as suitable conductive transparent electrode for solar cells. It is reported by many research works, that ZnO n-type doping is easier than p-type doping due to the self-compensation phenomena of intrinsic donors with acceptors [12]. Some studies have

been conducted on p-doped ZnO with N, P, Na, Ag, Cu, As and Li [13-19]. The efficiency of the p-doping of ZnO depends on the states occupied by the doping defects in the band gap and, their position in the lattice (substitutional or interestial sites). It is reported that group I elements such as lithium may have an acceptor behavior when substituting Zn sites or a donor behavior when occupying interstitial sites [20,21] leading to a doping limitation. Moreover, lithium should have low acceptor levels to be suitable for ZnO p-type doping. Park et al have reported ionization energy of 0.09 eV for substitutional Li [12]. Zaharescu et al. have also reported that the doping type may depend on the substrate used [10]. They have obtained p-type behavior for Li-doped ZnO deposited on silicon substrate and n-type behavior for ZnO deposited on glass substrate. They have argued that probably the glass substrate favors Li interstitial doping. The Li-doped ZnO thin films are useful for device fabrication in broadband UV photo-detectors for high tunable wavelength resolution

In this work, we report on Li-doped ZnO thin films elaborated with sol-gel spin coating. The influence of the Li-doping level on the ZnO structural, optical and electrical properties is presented. In particular, we study the effect of the lithium concentration on ZnO properties.

*Corresponding author: Wannes HB, Photovoltaic Laboratory, Center for Research and Energy Technologies, Borj-Cedria Technopole, Tunisia, Tel: (+216) 79 325 160; E-mail: benwannes.haifa00@gmail.com

Experimental Details

Fabrication procedure

Doped and undoped Zinc oxide thin films were deposited onto glass substrates by a spin-coating method. For solution preparation sol of Zinc acetate dihydrate ($Zn(CH_3COO)_2.2H_2O$) was prepared in boiling iso-proponal. This was followed by clearing the turbid solution by adding few drops of diethanolamine (DEA).

Lithium carbonate (Li_2CO_3) was used as a source of Li and a drop of nitric acid. The molar ratio of Li in the solution ([Li]/[Zn]) was varied: 0%, 5%, 15% and 25%. Finally, a clear homogeneous solution was obtained. These solutions were stirred (aged) for 24 hours at room temperature. Undoped ZnO and Li-doped ZnO thin films were prepared by a spin-coating method on cleaned and dried glass substrates. The solution was spin-coated on the substrates with the speed of 3000 rpm for 30 s. All prepared samples were subjected to a pre-heat treatment at 100°C for 10 minutes. This process of coating and heating was repeated 10 times. Finally, samples were annealed in a muffle furnace at 500°C for two hours under air. The obtained films were uniform, smooth and have a good adherence to the substrates.

Characterization techniques

Structural properties of ZnO thin films were obtained at room temperature using X-ray diffraction (XRD) "PAN alytical X'pert Pro MPD" diffractometer equipped with a copper Kα (λ=0.154 nm) radiation source and Fourier transformed infrared IR (FTIR) spectroscopy. Optical studies were performed by measuring the transmittance and the reflectance for wavelengths in the range of 200-2000 nm at room temperature using a Shimadzu UV-Vis 900 spectrophotometer. Photoluminescence measurements were carried out at ambient temperature with a 300 nm laser.

Results and Discussions

Structural properties

The X-Ray diffraction patterns of undoped and Li-doped ZnO thin films prepared by Sol-gel spin-coating are presented in Figure 1. The diffraction peaks, which correspond to (100), (002), (101), (102), (110) and (103) of ZnO, indicated that the sample was polycrystalline. However, with an additional increase in the Li concentration, these peaks [(102), (110) and (103)] are disappearing. The sample of 15.0 at % Li-doping concentration was polycrystalline with cubic phase. It is also worth noting that no peak related to lithium oxide has been found in the spectra, which may be due to the low Li content. We also note a gap of peak (100) towards the right with the increase of the concentration of Li which means that there are constraints of samples [22]. For thin films prepared at 25% the structures seem to be amorphous.

The structural parameters of undoped and doped ZnO:Li thin films are determined using the XRD results. The interplanar spacing d_{hkl} of different films were calculated using Bragg equation [23].

The lattice parameters "a" and "c" are calculated via (002) and (100) orientation using the following relation [24-25]:

$$\frac{1}{d_{hkl}^2} = \frac{4}{3a^2}(h^2 + k^2 + hk) + \frac{l^2}{c^2} \tag{1}$$

In cubic structure, the plane spacing is related to the lattice constant (a) and the Miller indices by the following relation:

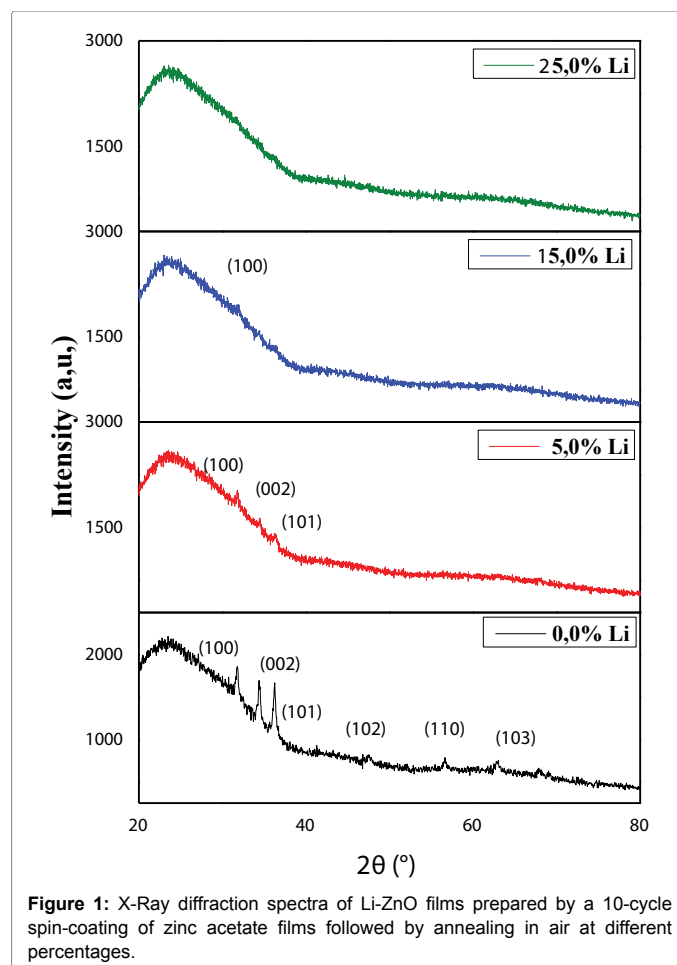$$\frac{1}{d_{hkl}^2} = \frac{h^2 + k^2 + l^2}{a^2} \tag{2}$$

Figure 1: X-Ray diffraction spectra of Li-ZnO films prepared by a 10-cycle spin-coating of zinc acetate films followed by annealing in air at different percentages.

The grain size D for different samples is estimated from the (002) diffraction peak using Debye–Scherer formula [25-27].

Where k=0.90 is the Scherer constant, $\beta_{1/2}$ is the full width at half maximum of peaks, is the Bragg angle corresponding to the peak and λ=1.54 A° is the X-ray wavelength. Figure 2 shows a decrease in the grain size as a function of increasing of the lithium content for concentrations 5% and 15%. This is may be due to the fact that lithium has a strong tendency to form Li_xO_y phases. The excess of Li atoms is located on the surface of ZnO. This observation is verified by the SEM images of pure and Li doped ZnO. This process is explained by the presence of an inward stress from the outside, which decreases the grain size.

Then, the microstrain ξ which is an interesting structural parameter of ZnO:Li thin films is calculated using the following relation [28]

$$\xi = \frac{\beta_{1/2}}{4 \tan \theta}. \tag{3}$$

Where $\beta_{1/2}$ is the full width at half-maximum of peaks and θ is the Bragg angle.

Finally, the dislocation density (δ) which is given by the following relation:

$$\delta = \frac{1}{D^2}. \tag{4}$$

This parameter increases from 0.93×10^{15} to 14.03×10^{15} lines/m² with Li content, as indicated in Table 1.

	d_{002}(Å)	d_{100}(Å)	a (Å)	c (Å)	D (nm)	ξ(10^{-4})	δ (10^{15}) lines/m^2
ZnO	2.6049	2.8152	3.25	5.209	36.33	36	0.96
ZnO : Li 5%	2.5608	2.2813	3.245	5.21	15.53	81.93	5.25
ZnO : Li 15%	-	2.808	2.808	-	8.44	149.8	14.03

Table 1: Different inter-planar spacing dhkl and the lattice constants of Li-ZnO thin films with different percentages.
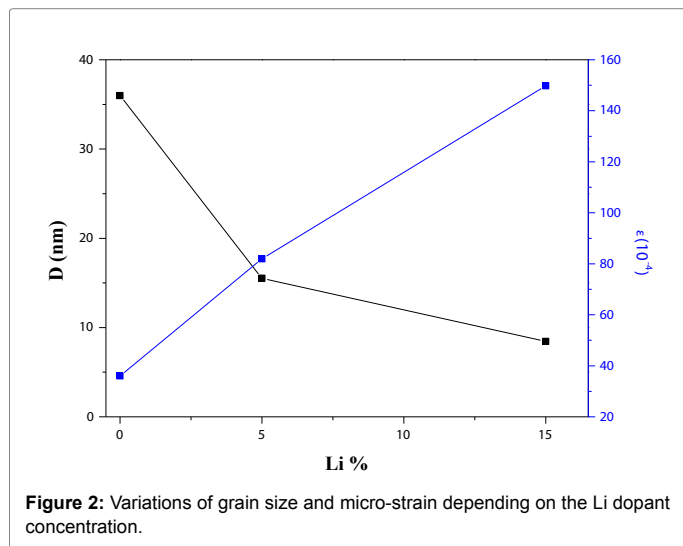

Figure 2: Variations of grain size and micro-strain depending on the Li dopant concentration.
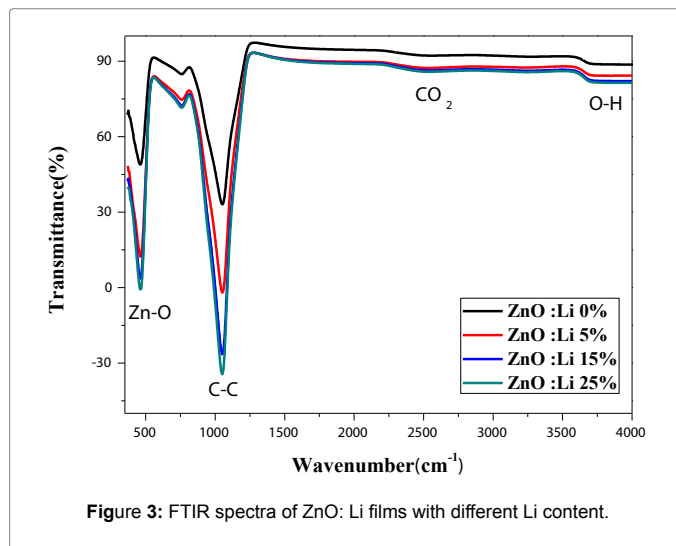

Figure 3: FTIR spectra of ZnO: Li films with different Li content.

Table 1 summarizes the values of d_{hkl} and the lattice constants for elaborated ZnO thin films. The 'a' and 'c' values were in concordance with the standard values of ZnO single crystal indicating the good crystalline quality of elaborated films. The interplanar spacing d_{hkl} decrease when the Li-doping concentration increases, we notice that the stress and the dislocation density increases, which leads to the decrease of the size of grains. The values for the 25% Li-doped samples are not presented as the films are amorphous.

Fourier transforms infrared (FTIR) analysis

Figure 3 presents the FTIR spectra of the samples of pure and doped Zn is recorded in the frequency band entre 400 cm^{-1}-4000 cm^{-1}. The band at ~1060 cm^1 appeared only in ZnO spectrum is related to C–C vibrations [29]. The broad band centered at ~3640 cm^{-1} is assigned to the O-H stretching vibrations, these vibrations are due to the presence of moisture [30] and another peak appeared at 2400 cm^{-1} is due to the existence of CO_2 in air or C–H bonds [31]. From these spectra, the effect of doping on the intensity of the Zn-O vibration band is observed. This band is very intense in the case of Li-doped ZnO (15% and 25%). The mid-height width and position of the Zn-O vibration band was influenced by the addition of Li^{2+} ions. Indeed, a small shift towards the low frequencies and a reduction in the width at mid-height was noted following the doping. This indicates the incorporation of Li^{2+} ions into the ZnO matrix.

Optical properties

UV analysis: The optical transmission, reflectance and absorbance spectra of ZnO: Li layers in 200-2000 nm domain are given in Figure 4a and 4b. The spectra show a high transmittance of all thin films, higher than 88%. This phenomenon can be attributed to less scattering effects, structural homogeneity and an improvement of the crystalline state.

Also, the absence of interference fringes in transmission spectra is due to the surface roughness caused by the spin-coating process. This is probably due to very small droplets resulting from this technique

between cycles of preparation this film [32]. In the same line, in the UV region, it can be seen shoulders, lying in transmission spectra which may be assigned to the presence of porosity and defaults inside the films.

It can also be seen that the interference fringe patterns are absent in all transmittance and reflectance spectra due to weak multiple reflection at the interface. This phenomenon can be contributed to more scattering effects and to the crystalline state. Then the reflectivity decrease with the increase of doping concentration, which proves that the elaborated films are transparent and they have a weak absorption. Within the visible and near IR range, the reflectance is negligible. Hence, the layer is anti-reflective. Finally, the highest transmission and the lowest reflectance are obtained for the oxide film prepared with a lithium percentage of 15% (Figure 5).

The band gap and the Urbach energies

a) Band gap energy calculation: The reflectance and transmission spectra present an accurate guide for estimating the absorption coefficient. When R (k) value is less than 30%, the absorption coefficient is given by [33]:

$$\alpha = \frac{1}{d} \ln(\frac{1}{T}). \tag{5}$$

Also, in the case of direct transmission, the absorption coefficient can be expressed by [33]:

$$(\alpha h \nu)^2 = [A(h \nu - E_g)]. \tag{6}$$

Where A is a constant, $h\nu$ is the photon energy and E_g is the optical band gap energy.

Figure 5 shows the plot of $[\alpha h\nu]^2$ versus the photon energy $h\nu$ which leads to the gap energy value in the sharp absorption edge by a linear fit. The results show a decrease in energy from 3.2 to 3.05 eV with the Lithium content. This band gap narrowing of transition metal doped II–IV semiconductor is likely to be interpreted in terms of sp-d
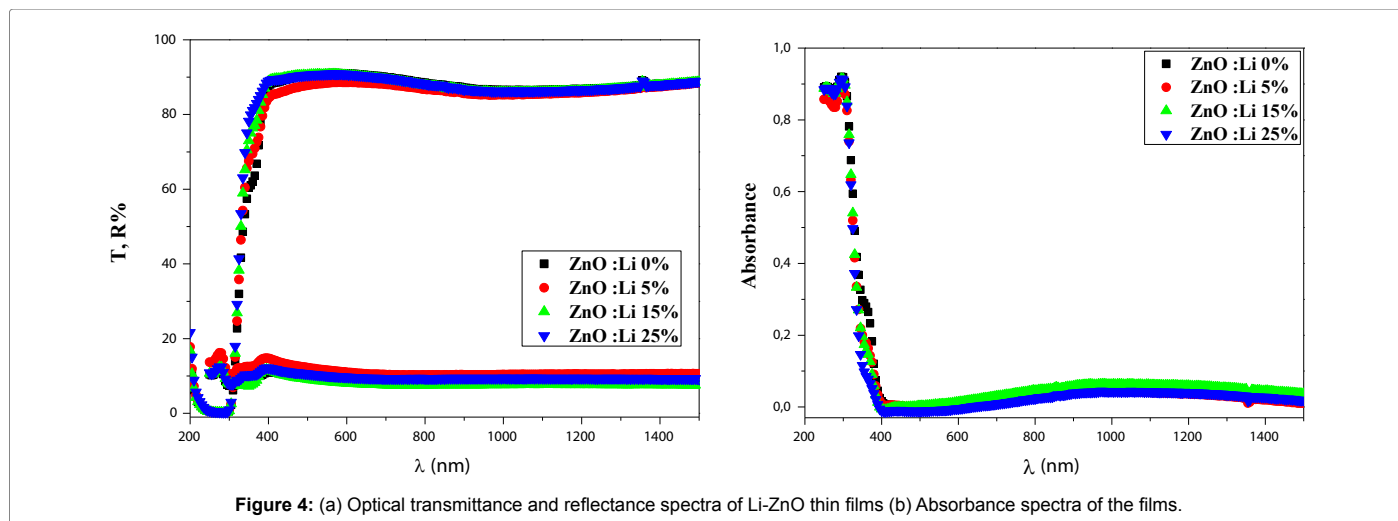
Figure 4: (a) Optical transmittance and reflectance spectra of Li-ZnO thin films (b) Absorbance spectra of the films.
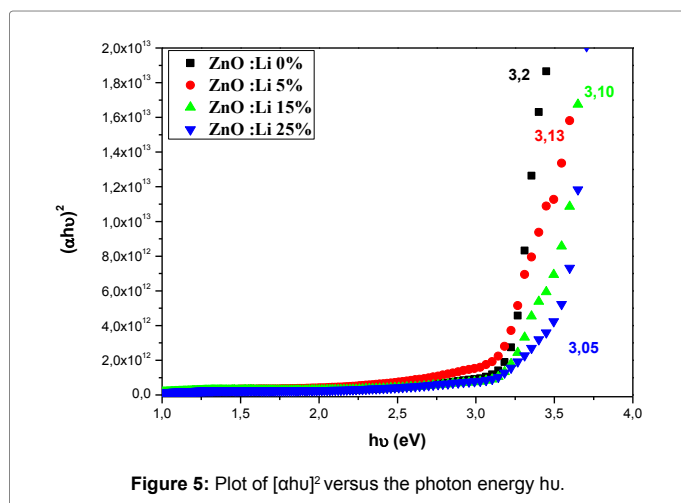

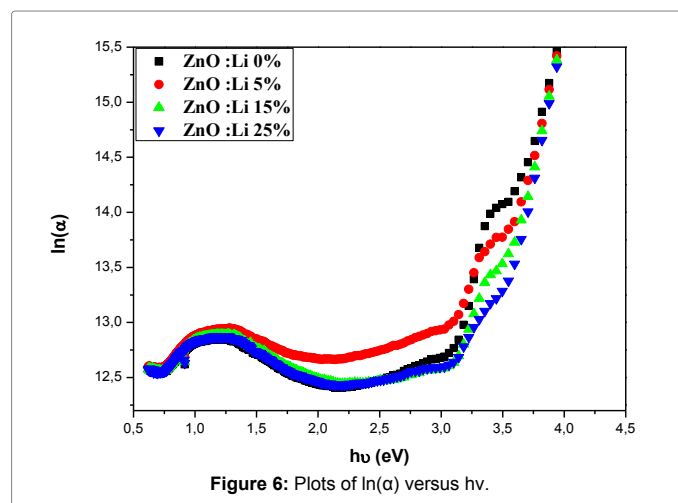**Figure 5:** Plot of $[\alpha h\upsilon]^2$ versus the photon energy $h\upsilon$.

Figure 6: Plots of $\ln(\alpha)$ versus $h\upsilon$.

	E_g (eV)	E_u (eV)
ZnO	3.2	0.239
ZnO: Li 5%	3.13	0.433
ZnO: Li 15%	3.1	0.444
ZnO: Li 25%	3.05	0.581

Table 2: Calculated values of band gap energy E_g and Urbach energy E_u.

spin exchange interactions between the conduction band electrons and the localized d electrons of transition metals ions Li^{2+}. Thus, the lithium doping did not alter the band gap much.

b) Urbach energy calculation: The Urbach energy tailing which characterizes the optical properties changes especially the optical absorption in the material follows the empirical Urbach law [34,35]. The Urbach energy Eu is obtained from the reverse of the slope of $\ln(\alpha)$ versus $h\upsilon$ [36].

We note that the Urbach energy increases by increasing the concentration of lithium; this suggests that the Li element is incorporated in the matrix. This calculation is in agreement with the calculation done for the dependence of the gap energy with lithium doping. Therefore, the disorder is promoted. The calculated values of optical band gap energy E_g and the Urbach energy Eu of ZnO:Li thin films as a function of Li content are summarized in Table 2.
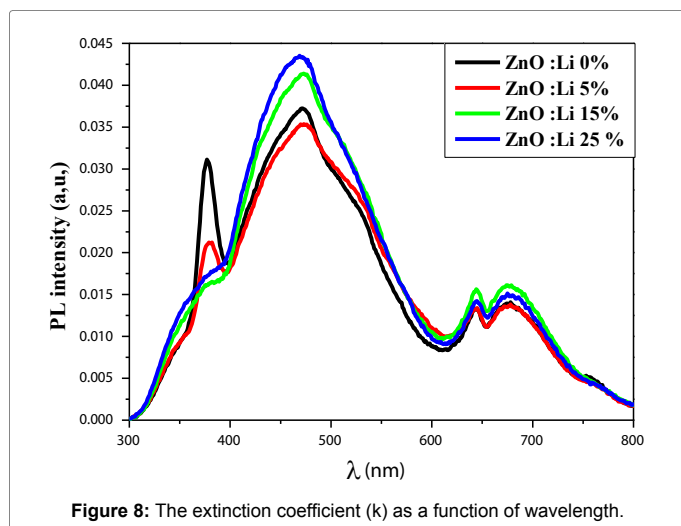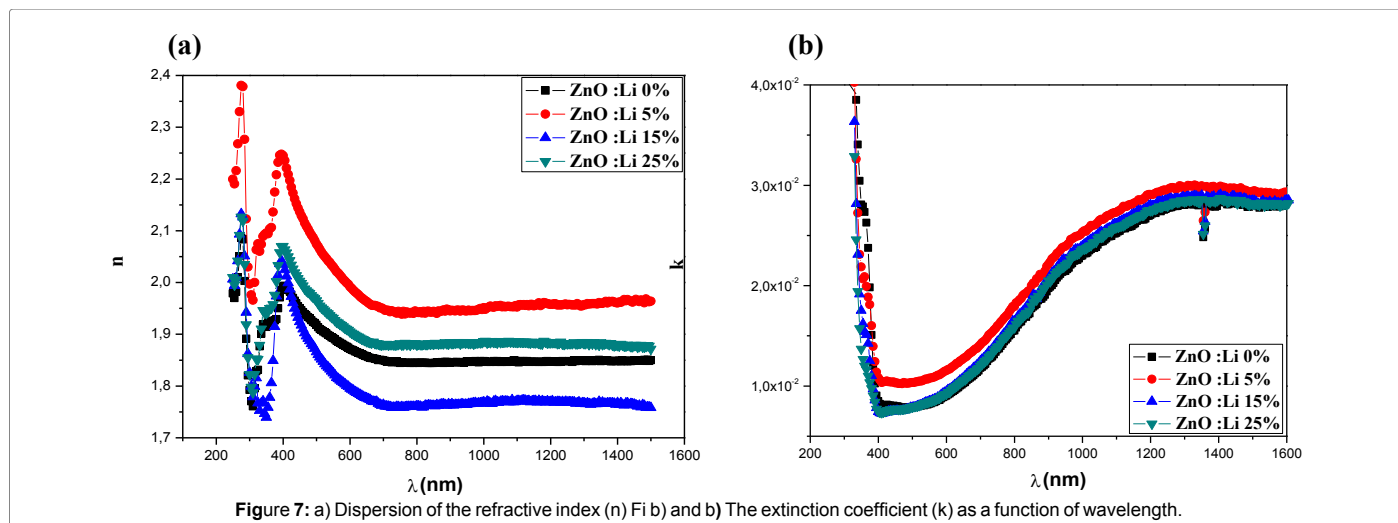
c) Refractive index and extinction coefficient: The optical dispersion coefficient $n(\lambda)$ and $k(\lambda)$, named refractive index and extinction coefficient respectively, for wavelength ranging from 200 to 2000 nm have been calculated using optical experimental measurements by means of methods [37-39]. The plots of $n(\lambda)$ and $k(\lambda)$ are presented in Figure 6

It is observed that the refractive index decreases especially for high wavelength with Li content.
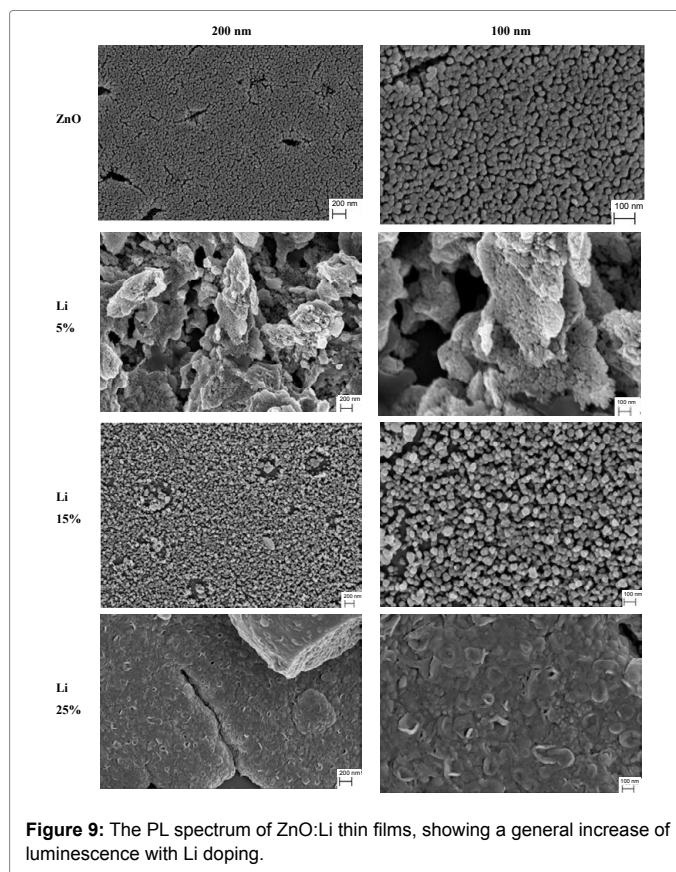
It is observed that the extinction coefficient k values decrease in the visible region can be attributed to the change of optical absorption of the films in the visible region, especially near UV range. Also, we note that the refractive index varies from 1.7 to 2.4 but the extinction coefficient belongs to $[5 \times 10^{-3}, 4 \times 10^{-2}]$ range Figures 7a and 7b.

PL analysis

The optical properties of the pure and Li-doped ZnO thin films were investigated by photoluminescence (PL) spectroscopy, which were excited by a laser radiation avoid, at room temperature. The PL spectra were obtained for the pure ZnO, 5%, 15% and 25% Li doped ZnO thin films. All the PL spectra consist of two emission bands and a shoulder at 640 nm located in UV and visible ranges (Figure 8). The spectrum of the PL of ZnO thin films undoped revealed a strong luminescence band

Figure 7: a) Dispersion of the refractive index (n) Fi b) and b) The extinction coefficient (k) as a function of wavelength.

Figure 8: The extinction coefficient (k) as a function of wavelength.

Figure 9: The PL spectrum of ZnO:Li thin films, showing a general increase of luminescence with Li doping.

at around 376 nm in the range of UV, corresponding to free exciton recombination and trapped impurities, at an energy close to that of the band gap of strong luminescence band of ZnO [40]. The decrease of near-band-edge (NBE) at around 376 nm is followed by the increase of deep-level (DL) emission is related to a radiative transition from donors to acceptors. As can be seen, the intensity of this peak decreased with lithium doping (5%), that can be attributed to filling some of Zn vacancies with Li^{2+} substitutional, which leads to becoming intrinsic n-type ZnO to p-type [41] and has disappeared completely when the lithium atoms of insertion in the ZnO matrix for other lithium percentages of 5%; This behavior can be attributed to the increase of the non-radiative centers caused by the existence of strong valence of the lithium (Li^{2+}) [42]. The broad emission band located in the visible range (400-700 nm) is mainly due to point-like structural defects related to deep-level emissions, such as zinc vacancies, oxygen vacancies, interstitial zinc, and interstitial oxygen, with a shoulder yellow-orange emission. For important concentrations of doping (15 and 25 % Li), the emission of the deep levels dominates specters PL and their intensity increases, its high intensity is a characteristic required for optoelectronic applications [43]. The incorporation of Li^{2+} is difficult due to the presence of native defects in ZnO lattice may cause the formation of different intrinsic defects which lead to the improved visible emission [44]. Such a behavior was brought reported in the p-type ZnO films [45].

Surface morphology

SEM images of undoped and doped ZnO thin films on glass substrates are presented in Figure 9. In the case of undoped ZnO films, the film presents a compact surface covered with uniform and mainly hexagonal grains with a size of 20-40 nm [46]. It was found also that, for undoped ZnO film, the surface was rough and crystal grain looked small; while, when the concentration of Lithium increase, we observe clusters of irregularly shaped grains and became bigger, its distribution and her surface uneven.

Conclusion

The effect of Li content on the physical properties of ZnO thin films has been investigated. First, XRD study shows that all ZnO:Li thin films coated are in polycrystalline hexagonal wurtzite state (with preferential c-axis orientation). Second, the optical band gap energy (3.05-3.2 eV) and the Urbach energy are calculated from optical absorption curves from 240 meV to 581 meV. It is found that both structural and optical properties of ZnO:Li thin films depend on the lithium content. The spectrum of the PL of ZnO thin films undoped revealed a strong luminescence band at around 376 nm in the field of UV which has disappeared when the lithium atoms of insertion in the ZnO matrix. The Photoluminescence study shows an increase in the visible emission. For important concentrations of Li doping, the emission of the deep levels dominates specters PL. Thin films could be used as light-emitting devices in optoelectronic applications as well as fabrication in broadband UV photo-detectors for high tunable wavelength resolution.

References

1. Fortunato E, Goncalves A, Marques A, Viana A, Aguas H, et al (2004) New developments in gallium doped zinc oxide deposited on polymeric substrates by RF magnetron sputtering. Surface and Coatings Technology 180-181: 20-25.

2. Smith FA, Baumard JF, Caillaud F (1992) Additives content in ZnO films prepared by spray pyrolysis. Research Gate 9: 447-452.

3. Seeber WT, Abou- Helal MO, Bath S, Beil D, Hoche T (1999) Transparent semiconducting ZnO:Al thin films prepared by spray pyrolysis. Materials Science in Semiconductor Processing 2: 45-55.

4. Moustaghfir A, Tomasella E, Amor BS, Jcquet M, Cellier J (2003) Structural and optical studies of ZnO thin films deposited by r.f. magnetron sputtering: influence of annealing. Surface and Coatings Technology 174: 193-196.

5. Haga K, Kamidaira M, Kashiwaba Y, Sekiguchi T, Watanabe H (2000) ZnO thin films prepared by remote plasma-enhanced CVD method. Journal of Crystal Growth 214-215: 77-80.

6. Narasimhan KL, Pai SP, Palkar VR, Pinto R (1997) High quality zinc oxide films by pulsed laser ablation. Thin Solid Films 295: 104-106.

7. Jlassi M, Sta I, Hajji M, Ezzaouia H (2014) Effect of nickel doping on physical properties of zinc oxide thin films prepared by the spray pyrolysis method. Applied Surface Science 301: 216-224.

8. Bao D, Gu H, Kuang A (1998) Sol-gel-derived c-axis oriented ZnO thin films. Thin Solid Films 312: 37-39.

9. Shakti N, Gupta PS (2010) Structural and Optical Properties of Sol-gel Prepared ZnO Thin Film. Applied Physics Research 2: 19-28.

10. Zaharescu M, Mihaiu S, Toader A, Atkinson I, Calderon-Moreno J, et al. (2014) ZnO based transparent conductive oxide films with controlled type of conduction. Thin Solid Films 571: 727-734.

11. Look DC (2001) Recent advances in ZnO materials and devices. Materials Science and Engineering B 80: 383-387.

12. Park CH, Zhang SB, Wei SH (2002) Origin of p-type doping difficulty in ZnO: The impurity perspective. Physical Review B 66: 073202.

13. Nian H, Hahn SH, Koo KK, Shin EW, Kim EJ (2009) Sol-gel derived N-doped ZnO thin films. Materials Letters 63: 2246-2248.

14. Kwon BJ, Kwack HS, Lee SK, Cho YH, Hwang DK, Park SJ (2007) Optical investigation of pp-type ZnO epilayers doped with different phosphorus concentrations by radio-frequency magnetron sputtering. Applied Physics Letters 91: 061903.

15. Lai JJ, Lin YJ, Chen YH, Chang HC, Liu CJ, et al (2011) Effects of Na content on the luminescence behavior, conduction type, and crystal structure of Na-doped ZnO films. Journal of Applied Physics 110: 013704.

16. Kim IS, Jeong EK, Kim DY, Kumar M, Choi SY (2009) Investigation of p-type behavior in Ag-doped ZnO thin films by E-beam evaporation. Applied Surface Science 255: 4011-4014.

17. Ahn KS, Deutsch T, Yan YF, Jiang CS, Perkins CL, et al. (2007) Synthesis of band-gap-reduced p-type ZnO films by Cu incorporation. Journal of Applied Physics 102: 023517.

18. Sun MH, Zhang QF, Wu JL (2007) Electrical and electroluminescence properties of As-doped p-type ZnO nanorod arrays. Journal of Physics D: Applied Physics 40: 3798.

19. Zeng YJ, Ye ZZ, Xu WZ, Chen LL, Li DY, et al. (2005) Realization of p-type ZnO films via monodoping of Li acceptor. Journal of Crystal Growth 283: 180-184.

20. Janotti A, Van de Walle CG (2009) Fundamentals of zinc oxide as a semiconductor. Reports on Progress in Physics 72: 126501.

21. Prakash C, Gaur A, Kumar A, Gaur UK (2014) Structural, morphological and optical study of Li doped ZnO thin films on Si (100) substrate deposited by pulsed laser deposition. Ceramics International 40: 11915-11923.

22. Boudjouan F, Chelouche A, Touam T, Djouadi D, Mahiou R, et al. (2016) Doping effect investigation of Li-doped nanostructured ZnO thin films prepared by sol–gel process. Journal of Materials Science: Materials in Electronics 27: 8040-8046.

23. Lupan O, Pauporte T, Chow L, Viana B, Pelle F, et al. (2010) Effects of annealing on properties of ZnO thin films prepared by electrochemical deposition in chloride medium. Applied Surface Science 256: 1895-1907.

24. Peng LP, Fang L, Yang XF, Li YJ, Huang QL, Wu F, et al. (2009) Effect of annealing temperature on the structure and optical properties of In-doped ZnO thin films. Journal of Alloys and Compounds 484 : 575-579.

25. Boukhachem A, Ouni B, Karyaoui M, Madani A, Chtourou R, et al. (2012) Structural, opto-thermal and electrical properties of ZnO:Mo sprayed thin films. Materials Science in Semiconductor Processing 15: 282-292.

26. Tripathi R, Kumar A, Bharti C, Sinha TP (2010) Dielectric relaxation of ZnO nanostructure synthesized by soft chemical method. Current Applied Physics 2: 676-681.

27. Junaid S, Qazi S, Adrian RR, Jeremy KC, Martin V (2009) Use of wide-angle X-ray diffraction to measure shape and size of dispersed colloidal particles. Journal of Colloid and Interface Science 1: 105-110.

28. Sahay PP, Nath RK (2008) Al-doped ZnO thin films as methanol sensors. Sensors and Actuators B: Chemical 134: 654-659.

29. Avci N, Smet J, Lauwaert H, Vrielinck D, Poelman J (2011) Optical and structural properties of aluminium oxide thin films prepared by a non-aqueous sol–gel technique. Journal of Sol-Gel Science and Technology 59: 327-333.

30. Lavrov EV, Weber J, Borrnert F, (2002) Hydrogen-related defects in ZnO studied by infrared absorption spectroscopy. SpringerLink, pp: 133-144.

31. Ozer N, Cronin JP, Yao YJ (1999) Optical Properties of Sol-Gel Deposited Al2o3 Films. Solar Energy Materials & Solar Cells 59: 355-360.

32. Wang L, Meng L, Teixeira V, Song S, Xu Z, et al. (2009) Structure and optical properties of ZnO:V thin films with different doping concentrations. Thin Solid Films 517: 3721-3725.

33. Caglar M, Ilican S, Caglar Y (2009) Influence of dopant concentration on the optical properties of ZnO: In films by sol-gel method. Thin Solid Films 517: 5023-5028.

34. Urbach F (1953) The Long-Wavelength Edge of Photographic Sensitivity and of the Electronic Absorption of Solids. Physical Review Journals Archive 92: 1324.

35. Martienssen W (1957) Über die excitonenbanden der alkalihalogenidkristalle. Journal of Physics and Chemistry of Solids 4: 257-267.

36. Ilican S, Caglar Y, Caglar M (2008) Preparation and characterization of ZnO thin films deposited by sol-gel spin coating method. Journal of Optoelectronics and Advanced Materials 10: 2578-2583.

37. Pankove JI (1971) Optical Processes in Semiconductors. Dover, New York, NY, USA.

38. Chopra Kasturi L (1969) Thin Film Phenomena. McGraw-Hill, New York 864p.

39. Caglar M, Ilican S, Caglar Y (2009) Influence of dopant concentration on the optical properties of ZnO: In films by sol–gel method. Thin Solid Films 517: 5023-5028.

40. Bousslama W, Elhouichet H, Gelloz B, Sieber B, Addad A, et al. (2012) Structural

and Luminescence Properties of Highly Crystalline ZnO Nanoparticles Prepared by Sol–Gel Method. Japanese Journal of Applied Physics 51: 04DG13.

41. Bagheri N, Majles AMH, Ghazyani N (2016) Characterization and doping effects study of high hole concentration Li-doped ZnO thin film prepared by sol–gel method. Journal of Materials Science: Materials in Electronics 27: 1293-1298.

42. Azizar RM, Phillips MR, That CT (2017) Efficient multi-coloured Li-doped ZnO thin films fabricated by spray pyrolysis. Journal of Alloys and Compounds 691: 339-342.

43. Arshad M, Ansari MM, Ahmed A, Tripathi P, Ashraf SSZ, et al. (2015) Band gap engineering and enhanced photoluminescence of Mg doped ZnO nanoparticles synthesized by wet chemical route. Journal of Luminescence 161: 275-280.

44. Djurišić AB, Leung YH (2006) Optical Properties of ZnO Nanostructures. Small Nano Micro 2: 944-961.

45. Sdiri N, Elhouichet H, Azeza B, Mokhtar F (2013) Studies of (90-x) P_2O_5-xB_2O_3-10Fe_2O_3 glasses by Mossbauer effect and impedance spectroscopy methods. Journal of Non-Crystalline Solids 37-372: 22-27.

46. Bayoud S, Addou M, Bahedi K, Jouad MEl, Sofiani Z, et al. (2013) The lithium effect on the blue and red emissions of Er-doped zinc oxide thin films. Physica Scripta T157: 014045.